

# Solution NMR Studies of a 42 kDa *Escherichia Coli* Maltose Binding Protein/β-Cyclodextrin Complex: Chemical Shift Assignments and Analysis

Kevin H. Gardner,\*†,§ Xiaochen Zhang,‡,|| Kalle Gehring,‡ and Lewis E. Kay\*,†

Contribution from the: Protein Engineering Network Centres of Excellence and Departments of Medical Genetics and Microbiology, Biochemistry, and Chemistry, University of Toronto, Toronto ON M5S 1A8 Canada, and Department of Biochemistry and Montreal Joint Centre for Structural Biology, McGill University, Montreal QC H3G 1Y6 Canada

Received June 9, 1998. Revised Manuscript Received September 25, 1998

**Abstract:** The use of deuteration in concert with uniform  $^{15}\text{N}$ ,  $^{13}\text{C}$ -labeling has been critical for the chemical shift assignment of several proteins and protein complexes over 30 kDa. Unfortunately, deuteration reduces the number of interproton distance restraints available for structure determination, compromising the precision and accuracy of the NMR-derived structures determined from these samples. We have recently described an isotopic labeling strategy that addresses this problem by generating proteins labeled uniformly with  $^{15}\text{N}$ ,  $^{13}\text{C}$ , and extensively with  $^2\text{H}$  with high levels of protonation at exchangeable sites and the methyl groups of Val, Leu, and Ile ( $\delta_1$  only) (Gardner, K. H.; Kay, L. E. *J. Am. Chem. Soc.* **1997**, *119*, 7599–7600). This labeling pattern maintains the high efficiency of triple resonance methods while retaining sufficient protons to establish long-range NOEs between secondary structure elements. We demonstrate the utility of samples labeled in this manner by presenting the chemical shift assignments of one of the largest monomeric proteins assigned to date, the 370 residue *Escherichia coli* maltose binding protein in complex with β-cyclodextrin (42 kDa). The high level of  $\text{C}\alpha$  and  $\text{C}\beta$  deuteration provided by our labeling scheme enabled the collection of triple resonance data with high sensitivity and resolution, allowing assignment of over 95% of the backbone  $^{15}\text{N}$ ,  $^{13}\text{C}\alpha$ ,  $^1\text{H}$ , and side chain  $^{13}\text{C}\beta$  nuclei. By using a combination of existing experiments and a new pulse scheme described here for correlating methyl chemical shifts with  $^{13}\text{C}\beta$  (Val),  $^{13}\text{C}\gamma$  (Leu), or  $^{13}\text{C}\gamma_1$  (Ile) carbons, over 98% of methyl  $^{13}\text{C}$  and  $^1\text{H}$  assignments from Val, Leu, and Ile ( $\text{C}\delta_1$  only) have been obtained. Analysis of the backbone chemical shifts and qualitative HN exchange data have confirmed that the MBP/β-cyclodextrin complex has a secondary structure similar to that previously observed in a 1.8 Å crystal structure.

## Introduction

Over the past forty years, solution NMR spectroscopy has emerged as a powerful technique for the study of macromolecular structure and dynamics. To successfully apply this methodology to progressively larger and more complex systems, it has been necessary to develop combinations of new isotopic labeling strategies and NMR pulse sequences to address problems with spectral resolution and sensitivity. For example, poor chemical shift dispersion and small homonuclear coupling constants restrict  $^1\text{H}$  NMR-based studies of protein structure to relatively small systems under 100 amino acids.<sup>1</sup> This limit was extended approximately 2-fold through the subsequent development of heteronuclear triple resonance NMR methods optimized for application to uniformly  $^{15}\text{N}$ ,  $^{13}\text{C}$ -labeled protein samples.<sup>2</sup> Although chemical shift assignments have been obtained for a number of fully protonated  $^{15}\text{N}$ ,  $^{13}\text{C}$ -labeled pro-

teins larger than 25 kDa,<sup>3–6</sup> rapid aliphatic  $^{13}\text{C}$  relaxation rates limit the sensitivity, and hence the utility, of many triple resonance methods.

Deuterium labeling significantly alleviates the molecular weight limitations associated with NMR studies of fully protonated  $^{15}\text{N}$ ,  $^{13}\text{C}$ -labeled proteins since  $^2\text{H}$  substitution reduces the magnitude of carbon–hydrogen dipolar interactions that dominate aliphatic  $^{13}\text{C}$  relaxation processes in protonated molecules.<sup>7</sup> The increase in carbon relaxation times associated with deuteration thus restores the sensitivity of triple resonance methods that transfer magnetization through carbon nuclei.<sup>8–11</sup> As such, many triple resonance methods have been modified

(3) Remerowski, M. L.; Domke, T.; Groenewegen, A.; Pepermans, H. A. M.; Hilbers, C. W.; van den Ven, F. J. M. *J. Biomol. NMR* **1994**, *4*, 257–278.

(4) Fogh, R. H.; Schipper, D.; Boelens, R.; Kaptein, R. *J. Biomol. NMR* **1995**, *5*, 259–270.

(5) Pham, T. N.; Koide, S. *J. Biomol. NMR* **1998**, *11*, 407–414.

(6) Copie, V.; Battles, J. A.; Schwab, J. M.; Torchia, D. A. *J. Biomol. NMR* **1996**, *7*, 335–340.

(7) Browne, D. T.; Kenyon, G. L.; Packer, E. L.; Sternlicht, H.; Wilson, D. M. *J. Am. Chem. Soc.* **1973**, *95*, 1316–1323.

(8) Yamazaki, T.; Lee, W.; Arrowsmith, C. H.; Muhandiram, D. R.; Kay, L. E. *J. Am. Chem. Soc.* **1994**, *116*, 11655–11666.

(9) Nietlispach, D.; Clowes, R. T.; Broadhurst, R. W.; Ito, Y.; Keeler, J.; Kelly, M.; Ashurst, J.; Oschkinat, H.; Domaille, P. J.; Laue, E. D. *J. Am. Chem. Soc.* **1996**, *118*, 407–415.

(10) Grzesiek, S.; Anglister, J.; Ren, H.; Bax, A. *J. Am. Chem. Soc.* **1993**, *115*, 4369–4370.

\* Author for correspondence.

† University of Toronto.

‡ McGill University.

§ Current address: Department of Biochemistry, University of Texas Southwestern Medical Center at Dallas, 5323 Harry Hines Blvd., Dallas, TX 75235-9038. Email: kgardn@biochem.swmed.edu.

|| current address: Spectral Diagnostics, Inc., 135-2 The West Mall, Toronto, ON M9C 1C2 Canada.

(1) Wüthrich, K. *NMR of proteins and nucleic acids*; John Wiley and Sons: New York, 1986.

(2) Bax, A. *Curr. Opin. Struct. Biol.* **1994**, *4*, 738–744.

for use with  $^2\text{H}$ ,  $^{15}\text{N}$ ,  $^{13}\text{C}$ -labeled protein samples.<sup>12</sup> The success of these methods has been amply demonstrated by the chemical shift assignments of several large proteins and protein complexes, including the protein components of two large Trp repressor/DNA complexes of 37 and 64 kDa,<sup>8,13</sup> the 340 residue MurB protein,<sup>14</sup> a 29 kDa rRNA methyltransferase,<sup>15</sup> the 29 kDa human carbonic anhydrase II protein,<sup>16</sup> and the 259 residue N-terminal domain from enzyme I of the *Escherichia coli* phosphoenolpyruvate:sugar phosphotransferase system.<sup>17</sup>

Unfortunately, while uniform  $^2\text{H}$  substitution does improve the sensitivity of many experiments, it also lowers the number of protons that can be used to obtain NOE-based distance restraints. In the limit of a fully deuterated protein, NOEs are only observed between pairs of exchangeable protons, chiefly those at backbone amide positions. Given the heavy reliance of current structure determination methods on internuclear distance restraints, decreasing their total number and distribution in this way can compromise the precision and accuracy of solution structures determined from highly deuterated proteins.<sup>18,19</sup> In light of this significant drawback, we have recently developed an isotopic-labeling method to generate highly deuterated proteins that are protonated in the methyl groups of Val, Leu, and Ile ( $\delta 1$  methyl group only) residues.<sup>20</sup> This labeling pattern maintains a sufficient level of deuteration to facilitate the collection of triple resonance spectra with high sensitivity and resolution while introducing protons at the methyl positions of hydrophobic residues that often bridge elements of secondary structure.<sup>21</sup> Long-range NOE-based restraints between methyl groups can be obtained from these samples that are critical for the determination of global protein folds.

Here we demonstrate the utility of the  $^{15}\text{N}$ ,  $^{13}\text{C}$ ,  $^2\text{H}$  ( $^1\text{H}$ -methyl)-labeling strategy that we have developed by reporting the chemical shift assignment of a 42 kDa complex of *E. coli* maltose binding protein (MBP, 370 residues) and a cyclic heptasaccharide,  $\beta$ -cyclodextrin. The uniformly high level of deuteration at the  $\text{C}\alpha$  and  $\text{C}\beta$  positions allowed the collection of triple resonance data with excellent sensitivity and resolution, facilitating the rapid assignment of virtually all of the backbone  $^{15}\text{N}$ ,  $^{13}\text{C}\alpha$ ,  $^1\text{H}$  and side chain  $^{13}\text{C}\beta$  chemical shifts of the 370 residue protein. The high level of protonation at the methyl positions of Val, Leu, and Ile ( $\text{C}\delta 1$  only) residues allowed the assignment of the methyl groups of these residues using sensitive experiments. An analysis of the backbone chemical shifts and HN exchange protection data has confirmed that the secondary structure of MBP in solution is similar to that observed in a crystal structure of the MBP/ $\beta$ -cyclodextrin complex. This work

establishes that solution NMR-based methods are capable of assigning the chemical shifts of large proteins, a prerequisite to any study of the structure or dynamics of such systems.

## Materials and Methods

Unless otherwise noted, all of the NMR experiments used samples of *E. coli* maltose binding protein (MBP) that were uniformly  $^{15}\text{N}$  and  $^{13}\text{C}$  labeled and extensively deuterated at aliphatic and aromatic positions except for the methyl groups of Val, Leu, and Ile ( $\delta 1$  methyl only) [referred to here as  $^{15}\text{N}$ ,  $^{13}\text{C}$ ,  $^2\text{H}$  ( $^1\text{H}$ -methyl)-labeling].<sup>20</sup>  $^{15}\text{N}$ ,  $^{13}\text{C}$ ,  $^2\text{H}$  ( $^1\text{H}$ -methyl)-labeled samples of MBP were generated by overexpression from cultures of *E. coli* strain BL21(DE3) transformed with the plasmid pmal-c0, which encodes residues 1–370 of mature MBP with substitution of Ile 2 by threonine and the addition of an N-terminal methionine (J.-M. Clement, private communication). Following transformation, MBP was produced from a bacterial culture grown using the scheme shown in Figure 1. Approximately 1 h pre-induction, 40 mg/L of [2,3- $^2\text{H}_2$ ] $^{15}\text{N}$ ,  $^{13}\text{C}$ -valine (see below) and 50 mg/L of [3,3- $^2\text{H}_2$ ] $^{13}\text{C}$   $\alpha$ -ketobutyrate were provided as precursors for deuterated, methyl-protonated forms of Val, Leu, and Ile. Purification of MBP was achieved using a combination of amylose affinity, anion-exchange, and size-exclusion chromatography, resulting in yields of approximately 20 mg/L. In comparing  $^{15}\text{N}$ – $^1\text{H}$  HSQC spectra recorded on these highly deuterated samples with spectra from fully protonated molecules, we noted that a significant number (>50) of backbone amide groups remained deuterated throughout the purification process (4 °C, 7–10 days). To fully protonate these sites, the protein was partially unfolded for 3 h at room temperature in a buffer containing 2.5 M guanidinium hydrochloride (GuHCl) and subsequently refolded by rapid dilution into GuHCl-free buffer containing 2 mM  $\beta$ -cyclodextrin. Two 300- $\mu\text{L}$  samples were prepared in this manner and contained either 0.7 or 0.9 mM MBP, 2 mM  $\beta$ -cyclodextrin, 20 mM sodium phosphate buffer (pH 7.2), 3 mM NaN<sub>3</sub>, 100  $\mu\text{M}$  EDTA, 0.1 mg/mL Pefabloc, 1  $\mu\text{g}/\text{mL}$  pepstatin, and 10% D<sub>2</sub>O.

Constant-time (CT) 2D  $^{13}\text{C}$ – $^1\text{H}$  HSQC<sup>22,23</sup> and CT- $\text{HN}(\text{COCA})\text{CB}$ <sup>13</sup> spectra of these samples, produced using 40 mg/L of [2,3- $^2\text{H}_2$ ] $^{15}\text{N}$ ,  $^{13}\text{C}$ -valine, established that the Val, Leu, and Ile  $\delta 1$  methyl groups were protonated to levels of approximately 85, 50, and 95%, respectively. More recent studies have shown that significantly higher levels of Val and Leu methyl protonation can be obtained by supplying the final bacterial culture with a larger quantity of [2,3- $^2\text{H}_2$ ] $^{15}\text{N}$ ,  $^{13}\text{C}$ -valine (unpublished results). For example, by adding 80 mg/L of valine 4 h prior to induction, we were able to generate samples of the MBP/ $\beta$ -cyclodextrin complex with 92 ± 2% (Val) and 88 ± 1% (Leu) methyl protonation. Alternatively, 50 mg/L of valine supplied 1 h pre-induction led to a sample with 88 ± 2% (Val) and 80 ± 2% (Leu) labeling, consistent with previous results.<sup>20</sup> In any regard, it is clear that greater than 40 mg/L of [2,3- $^2\text{H}_2$ ] $^{15}\text{N}$ ,  $^{13}\text{C}$ -valine must be added to ensure high level labeling of Val and Leu methyl groups (N. Goto et al., manuscript in preparation).

CT  $^{13}\text{C}$ – $^1\text{H}$  HSQC spectra also demonstrated that all of the protonated Val, Leu, and Ile  $\delta 1$  methyl groups are of the  $\text{CH}_3$  type, with no evidence of the partially protonated  $\text{CH}_2\text{D}$  and  $\text{CHD}_2$  isotopomers that had been observed in Val, Leu, and Ile residues of one previously prepared sample.<sup>24</sup> We attribute the absence of these unwanted isotopomers in the samples used in this work to a more complete dilution of the partially protonated bacteria at one of the transfer steps and the shorter induction time used for these samples (4 h, compared to 8 h). Using the protocol described in Figure 1, two other groups have also recently produced proteins free of partially deuterated isotopomers (R. A. Byrd, NCI, private communication; M. K. Rosen, Sloan Kettering, private communication). In this regard, it is worth mentioning that previous NMR studies that measured the level of proton incorporation at the methyl positions of Val, Leu, and Ile ( $\text{C}\delta 1$  only) established an isotopomer distribution of 92%  $\text{CH}_3$ /8%  $\text{CD}_3$  for Val and Leu, while for Ile >98%  $\text{CH}_3$ / $<2\%$   $\text{CD}_3$  was observed.<sup>20</sup>

(22) Santoro, J.; King, G. C. *J. Magn. Reson.* **1992**, 97, 202–207.

(23) Vuister, G. W.; Bax, A. *J. Magn. Reson.* **1992**, 98, 428–435.

(24) Zwahlen, C.; Vincent, S. J. F.; Gardner, K. H.; Kay, L. E. *J. Am. Chem. Soc.* **1998**, 120, 4825–4831.

(11) Farmer, B. T., II; Venters, R. A. *J. Am. Chem. Soc.* **1995**, 117, 4187–4188.

(12) For a review, see: Gardner, K. H.; Kay, L. E. *Annu. Rev. Biophys. Biomol. Struct.* **1998**, 27, 357–406.

(13) Shan, X.; Gardner, K. H.; Muhandiram, D. R.; Rao, N. S.; Arrowsmith, C. H.; Kay, L. E. *J. Am. Chem. Soc.* **1996**, 118, 6570–6579.

(14) Constantine, K. L.; Mueller, L.; Goldfarb, V.; Wittekind, M.; Metzler, W. J.; Yanuchas, J. J.; Robertson, J. G.; Malley, M. F.; Friedrichs, M. S.; Farmer, B. T., II. *J. Mol. Biol.* **1997**, 267, 1223–1246.

(15) Yu, L.; Petros, A. M.; Schnuchel, A.; Zhong, P.; Severin, J. M.; Walter, K.; Holzman, T. F.; Fesik, S. W. *Nat. Struct. Biol.* **1997**, 4, 483–489.

(16) Venters, R. A.; Farmer, B. T., II; Fierke, C. A.; Spicer, L. D. *J. Mol. Biol.* **1996**, 264, 1101–1116.

(17) Garrett, D. S.; Seok, Y.; Liao, D.; Peterkofsky, A.; Gronenborn, A. M.; Clore, G. M. *Biochemistry* **1997**, 36, 2517–2530.

(18) Venters, R. A.; Metzler, W. J.; Spicer, L. D.; Mueller, L.; Farmer, B. T., II. *J. Am. Chem. Soc.* **1995**, 117, 9592–9593.

(19) Gardner, K. H.; Rosen, M. K.; Kay, L. E. *Biochemistry* **1997**, 36, 1389–1401.

(20) Gardner, K. H.; Kay, L. E. *J. Am. Chem. Soc.* **1997**, 119, 7599–7600.

(21) Janin, J.; Miller, S.; Chothia, C. *J. Mol. Biol.* **1988**, 204, 155–164.

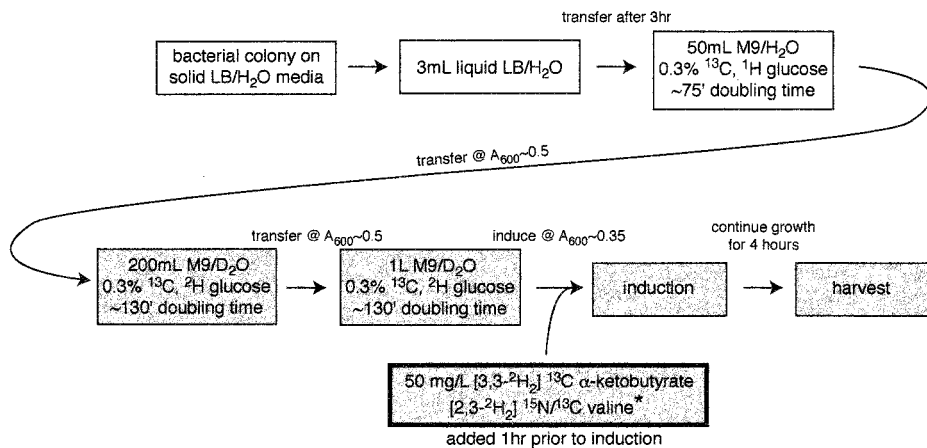


**Figure 1.** Growth scheme used to produce  $^{15}\text{N}$ ,  $^{13}\text{C}$ ,  $^2\text{H}$  ( $^1\text{H}$ -methyl)-labeled protein samples. All cultures were grown at  $37^\circ\text{C}$  with the indicated doubling times. All steps in M9 minimal media contained  $0.1\%$   $^{15}\text{NH}_4\text{Cl}$  and  $0.3\%$  glucose, with the listed isotopic composition, as the sole nitrogen and carbon sources, respectively. All isotopically labeled compounds (except  $\alpha$ -ketobutyrate, which was generated as described previously<sup>20</sup>) were purchased from Cambridge Isotope Labs. Transfer steps were achieved by briefly centrifuging (at  $20^\circ\text{C}$ ) a sufficient amount of the culture to start the next growth step with an  $A_{600} = 0.1$ , discarding the supernatant and resuspending the cell pellet in the listed volume of fresh media. As discussed in the Materials and Methods section, the concentration of  $[2,3-^2\text{H}_2]^{15}\text{N}, ^{13}\text{C}$ -valine (\*) added in this study (40 mg/L) was lower than optimal, resulting in only  $\sim 85\%$  (Val) and  $\sim 50\%$  (Leu) methyl protonation. We recommend the use of higher levels as described previously<sup>20</sup> and described in Materials and Methods. The timing of the addition of the  $\alpha$ -ketobutyrate/valine ( $\alpha$ -kb/Val) mixture is dependent on its volume: when prepared using our previously described method<sup>20</sup> these compounds are in a dilute mixture, composing a significant portion ( $\sim 20\%$ ) of the final volume of the bacterial culture after addition. As such, the  $\alpha$ -kb/Val mixture should be added at  $A_{600} \approx 0.35$ , initially diluting the culture but allowing it to return to this density during the following hour before induction. In contrast, by using commercially available labeled  $\alpha$ -ketobutyrate (Cambridge Isotope Labs), one can add the required amounts of  $\alpha$ -kb/Val in a smaller volume, diluting the bacterial culture to a lesser degree. In this case, these compounds should be added at  $A_{600} \approx 0.25$  (assuming a doubling time of 130 min) to account for growth of the bacterial culture in the following hour-long incubation. The  $\alpha$ -kb/Val mixture is provided in complete M9/D<sub>2</sub>O media, including  $0.1\%$   $^{15}\text{NH}_4\text{Cl}$  and  $0.3\%$  U-[ $^{13}\text{C}$ ,  $^2\text{H}$ ] glucose. Induction was triggered by the addition of 250 mg/L of IPTG. The approximate cost of the final labeling media (M9/D<sub>2</sub>O with  $^{15}\text{NH}_4\text{Cl}$ ,  $0.3\%$  U-[ $^{13}\text{C}$ ,  $^2\text{H}$ ] glucose and 80 mg/L of  $[2,3-^2\text{H}_2]^{15}\text{N}, ^{13}\text{C}$ -valine, and 50 mg/L of  $[3,3-^2\text{H}_2]^{13}\text{C}$   $\alpha$ -ketobutyrate) is \$3000/liter. Note that some cost savings can be achieved by recycling the D<sub>2</sub>O content of used media by flash distillation.

The isotopomer distribution observed for Val was confirmed in CT-HN(COCA)CB experiments, described below.

A [U- $^{15}\text{N}$ , U-10%  $^{13}\text{C}$ ] sample of MBP was also generated to facilitate the stereospecific assignment of Val and Leu methyl groups by the method of Neri et al.<sup>25</sup> This sample was produced by overexpression using a culture of BL21(DE3) cells transformed with the pmal-c<sub>0</sub> vector and grown in M9 media containing  $^{15}\text{NH}_4\text{Cl}$  and 10%  $^{13}\text{C}$ -enriched/90%  $^{13}\text{C}$ -natural abundance glucose. The sample was purified as described above.

All NMR experiments were performed on a four-channel Varian Inova 600 MHz spectrometer operating at  $37^\circ\text{C}$  and equipped with an actively shielded triple resonance probe with a Z-axis pulsed field gradient coil. Backbone chemical shift assignments were obtained by recording 3D CT-HNCA, CT-HN(CO)CA, CT-HN(CA)CB, and CT-HN(COCA)CB and HNCO experiments using previously described pulse sequences,<sup>8,13,26,27</sup> with the parameters indicated in Table 1 of the Supporting Information. Methyl  $^1\text{H}$  and  $^{13}\text{C}$  chemical shifts were obtained from a (H)C(CO)NH-TOCSY,<sup>28</sup> which has been optimized for application to highly deuterated, methyl-protonated samples, and H(C)(CO)NH-TOCSY and (H)C(CA)NH-TOCSY experiments, derived from the (H)C(CO)NH-TOCSY. In addition, a new pulse scheme, the (HM)CMC(CM)HM experiment, was developed to correlate the methyl  $^1\text{H}$  and  $^{13}\text{C}$  chemical shifts with the chemical shift of the immediately adjacent carbon. Details concerning the magnetization transfer steps of this pulse sequence will be described in Results and Discussion. The (HM)CMC(CM)HM data set was comprised of (49, 89, 576) complex points in each of ( $t_1$ ,  $t_2$ ,  $t_3$ ), corresponding to net acquisition

times of (13.6, 24.7, and 64.0 ms). Four scans per FID were recorded corresponding to a net acquisition time of 63 h. Acquisition parameters for all of the remaining side-chain experiments (which have been published previously) are listed in Table 1 of the Supporting Information. Val and Leu methyl groups were stereospecifically assigned from the relative phases of cross-peaks observed in  $^{13}\text{C}$ - $^1\text{H}$  CT-HSQC spectra<sup>25</sup> acquired on the [U- $^{15}\text{N}$ , U-10%  $^{13}\text{C}$ ] labeled MBP/ $\beta$ -cyclodextrin complex and recorded with a constant-time delay of  $1/J_{\text{CC}}$  ( $\sim 29$  ms), where  $J_{\text{CC}}$  is the one-bond  $^{13}\text{C}$ - $^{13}\text{C}$  coupling. Assignments were also facilitated by recording a CT-HSQC with a delay set to  $1.5/J_{\text{CC}}$ , so that only pro-S methyls are observed.<sup>29</sup>

All NMR spectra were processed using the NMRPipe package.<sup>30</sup> Details concerning processing of the constant-time triple resonance spectra for backbone assignment are similar to those given in Yamazaki et al.<sup>8</sup> and Shan et al.<sup>13</sup> Briefly, residual water in the acquisition dimension was minimized by a time-domain deconvolution procedure,<sup>31</sup> followed by apodization with a  $70^\circ$  shifted sine-squared window function, zero filling, Fourier transformation, phasing, and elimination of the imaginary component of the signal. The  $^{15}\text{N}$  dimension was doubled using mirror image linear prediction,<sup>32</sup> apodized with an  $80^\circ$  shifted sine-squared function, zero filled, Fourier transformed, and phased. The  $^{13}\text{C}$  dimension in each of these experiments was processed similarly, with the exception that the linear prediction step was omitted. The TOCSY-based side-chain experiments were processed in a manner similar to that of the backbone schemes, with the exception that forward-backward linear prediction<sup>33</sup> was employed in the  $^{13}\text{C}$  or  $^1\text{H}$  dimensions ( $F_1$ ), rather than in  $^{15}\text{N}$ . The methyl carbon dimension of the (HM)CMC(CM)HM data set was doubled using mirror image linear

(25) Neri, D.; Szyperski, T.; Otting, G.; Senn, H.; Wüthrich, K. *Biochemistry* **1989**, *28*, 7510–7516.

(26) Yamazaki, T.; Lee, W.; Revington, M.; Mattiello, D. L.; Dahlquist, F. W.; Arrowsmith, C. H.; Kay, L. E. *J. Am. Chem. Soc.* **1994**, *116*, 6464–6465.

(27) Kay, L. E.; Xu, G. Y.; Yamazaki, T. *J. Magn. Reson. A* **1994**, *109*, 129–133.

(28) Gardner, K. H.; Konrat, R.; Rosen, M. K.; Kay, L. E. *J. Biomol. NMR* **1996**, *8*, 351–356.

(29) Hu, W. D.; Zuiderweg, E. R. P. *J. Magn. Reson. B* **1996**, *113*, 70–75.

(30) Delaglio, F.; Grzesiek, S.; Vuister, G. W.; Zhu, G.; Pfeifer, J.; Bax, A. *J. Biomol. NMR* **1995**, *6*, 277–293.

(31) Marion, D.; Ikura, M.; Bax, A. *J. Magn. Reson.* **1989**, *84*, 425–430.

(32) Zhu, G.; Bax, A. *J. Magn. Reson.* **1990**, *90*, 405–410.

(33) Zhu, G.; Bax, A. *J. Magn. Reson.* **1992**, *100*, 202–207.

prediction, apodized with a 50 Hz Gaussian window, Fourier transformed, and phased, while the second carbon dimension was processed similarly but without linear prediction. After each of the transformed data sets were reduced to include only the spectral regions of interest, the spectra were analyzed using the program NMRView<sup>34</sup> in conjunction with Tcl scripts provided by Bruce Johnson or written in-house, designed to interface with the database facilities of NMRView.

The  $^{13}\text{C}\alpha/^{13}\text{C}\beta$  chemical shifts of MBP were analyzed using a hybrid approach based on the  $^{13}\text{C}$  chemical shift index<sup>35</sup> and the method of Metzler et al.<sup>36</sup> where  $(\Delta C^\alpha - \Delta C^\beta)_{\text{smoothed}}$  is calculated for each residue  $[(\Delta C^\alpha - \Delta C^\beta) = (^{13}\text{C}\alpha^{\text{obs}} - ^{13}\text{C}\alpha^{\text{rc}}) - (^{13}\text{C}\beta^{\text{obs}} - ^{13}\text{C}\beta^{\text{rc}})]$ , where obs and rc refer to the observed and residue-specific random coil chemical shifts, respectively. The table of random coil carbon chemical shifts provided by Wishart and Sykes<sup>35</sup> was corrected for  $^2\text{H}$ -isotope effects<sup>37</sup>—expected of a  $^2\text{H}$  ( $^1\text{H}$ -methyl)-labeled sample. The value,  $(\Delta C^\alpha - \Delta C^\beta)$ , was plotted as a function of residue, and a three-point binomial smoothing function was applied to generate the value  $(\Delta C^\alpha - \Delta C^\beta)_{\text{smoothed}}$  (see below). The locations of secondary structure elements were determined by identifying groups of residues with  $|(\Delta C^\alpha - \Delta C^\beta)_{\text{smoothed}}| > 1.4$  ppm and applying the  $^{13}\text{C}$  CSI empirical filtering rules.<sup>35</sup>

## Results and Discussion

**Backbone Assignments.** It is well established that the sensitivity of triple resonance experiments recorded on large proteins and protein complexes can be significantly improved through the use of  $^2\text{H}$ -labeled samples.<sup>12</sup> This improvement is based on the reduction of line widths of carbons that would normally be one-bond coupled to protons as well as a decrease in line widths of remaining protons, such as those at backbone amide positions.<sup>38</sup> For experiments which rely on magnetization transfer through proton-bearing carbon nuclei, such as those used to assign the  $\text{C}\alpha$  and  $\text{C}\beta$  chemical shifts in the MBP/β-cyclodextrin complex, this slowed relaxation resulting from the substitution of deuterons for protons translates into diminished magnetization losses. As such, high level deuteration of aliphatic carbon positions is particularly desirable and is achieved by the  $^{15}\text{N},^{13}\text{C},^2\text{H}$  ( $^1\text{H}$ -methyl)-labeling method (Figure 1). In particular, no significant protein resonances are visible in the chemical shift range typical of  $\text{H}\alpha$  or  $\text{H}\beta$  protons, as shown in Figure 2. In contrast, intense signals are observed in both the methyl and amide regions, resulting from the  $\alpha$ -ketobutyrate/valine-labeling procedure described in Figure 1 and the unfolding/refolding steps used to generate this sample. Note that complete protonation at the backbone amide protons is necessary for the use of the out-and-back type HN-detected triple resonance methods that have been developed for backbone chemical shift assignments of highly deuterated proteins.

Figure 3 illustrates the  $^{15}\text{N}-^1\text{H}$  HSQC spectrum of the  $^{15}\text{N},^{13}\text{C},^2\text{H}$  ( $^1\text{H}$ -methyl)-MBP/protonated β-cyclodextrin complex. The uniform intensities and line widths of cross-peaks throughout the spectrum indicate that there are no large regions involved in intermediate time scale exchange processes, although a more thorough analysis identified broadening of amide resonances located in two short sections of the protein near the bound β-cyclodextrin (see below).

As was observed in previous applications of the CT-triple resonance methodology,<sup>8,13</sup> high quality spectra with excellent

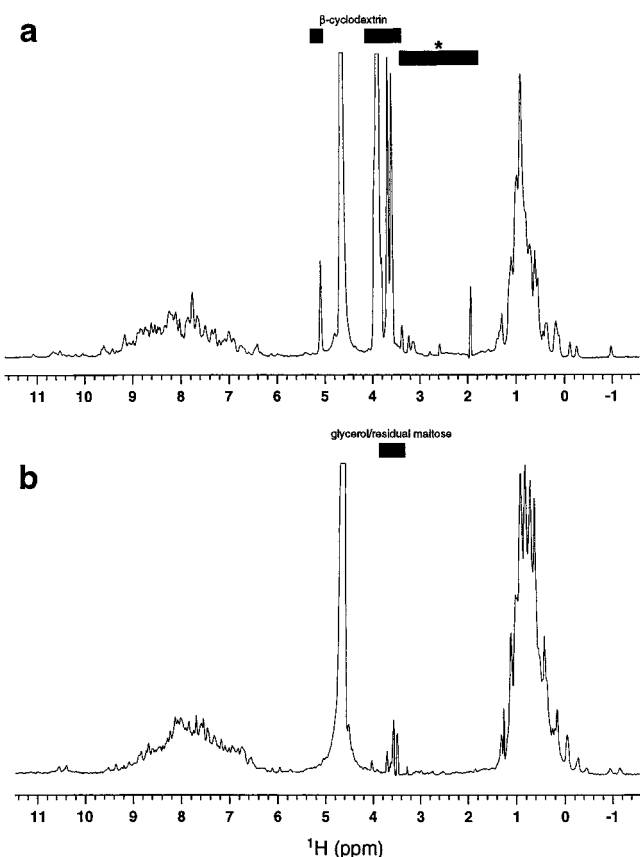


**Figure 2.** Specificity of protonation in  $^{15}\text{N},^{13}\text{C},^2\text{H}$  ( $^1\text{H}$ -methyl)-labeled samples. One-dimensional  $^1\text{H}$  NMR spectra were recorded of the  $^{15}\text{N},^{13}\text{C},^2\text{H}$  ( $^1\text{H}$ -methyl)-MBP/β-cyclodextrin complex (a, with  $^{15}\text{N},^{13}\text{C}$ -decoupling) and of free  $^{15}\text{N},^{13}\text{C},^2\text{H}$  ( $^1\text{H}$ -methyl)-MBP (b, no decoupling). Peaks from β-cyclodextrin (a) and glycerol or residual maltose (b) are located below the appropriately labeled black bars; the peaks identified with the black bar labeled with an asterisk in (a) originated from  $^{12}\text{C}$  contaminants that were not present in all samples.

sensitivity and resolution were obtained for the MBP/β-cyclodextrin complex. Backbone chemical shift assignments were made using an approach similar to that used to assign the protein components of a 64 kDa trp repressor/DNA complex.<sup>13</sup> It is likely that the sensitivity and resolution of spectra of the MBP/β-cyclodextrin complex (e.g., Figure 3) are better than would be expected for those of many proteins of similar molecular weight, facilitating the rapid assignment of the MBP backbone chemical shifts. Through the use of automated scripts provided with NMRView<sup>34</sup> combined with occasional manual intervention, one person was able to complete the bulk of the backbone assignments (>90%) in approximately 7 days. We anticipate that this time could be significantly decreased with the continued development of tools designed to automate the assignment process.

Figure 4 presents slices of CT-HNCA and CT-HN(CA)CB spectra used in the assignment of backbone chemical shifts for amino acids 28–39, which includes residues in α-helical, turn, and β-strand conformations. Despite the relatively low protein concentration (<1 mM) used to acquire these spectra, all of the possible inter- and intraresidue cross-peaks for the residues shown here are observed. (The  $^{13}\text{C}\alpha$  chemical shifts of E28 and K29 are degenerate, as are those of T36 and V37). The sensitivity of the correlations observed in Figure 4 is representative of the signal-to-noise observed throughout the bulk of the protein. Both inter- and intraresidue cross-peaks were obtained for 90.3% (HNCA) and 72.8% (HN(CA)CB) of the non-Pro

(34) Johnson, B. A.; Blevins, R. A. *J. Biomol. NMR* 1994, 4, 603–614.

(35) Wishart, D. S.; Sykes, B. D. *J. Biomol. NMR* 1994, 4, 171–180.

(36) Metzler, W. J.; Constantine, K. L.; Friedrichs, M. S.; Bell, A. J.; Ernst, E. G.; Lavoie, T. B.; Mueller, L. *Biochemistry* 1993, 32, 13818–13829.

(37) Hansen, P. E. *Prog. Nucl. Magn. Reson. Spectrosc.* 1988, 20, 207–255.

(38) Markus, M. A.; Kaye, K. T.; Matsudaira, P.; Wagner, G. *J. Magn. Reson. B* 1994, 105, 192–195.

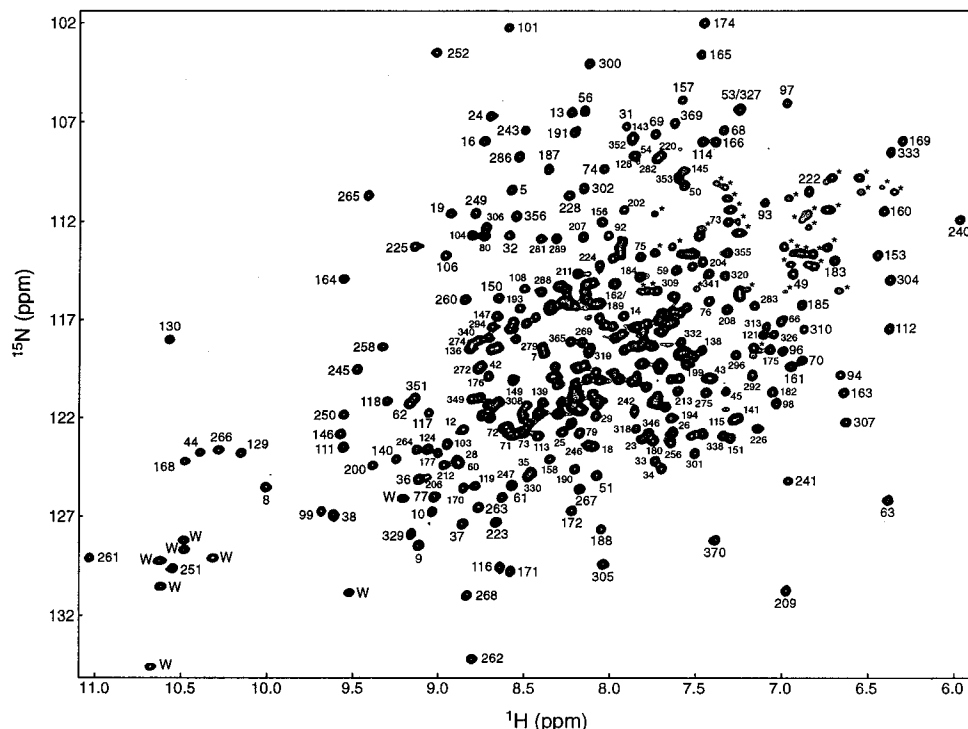


**Figure 3.**  $^{15}\text{N}-^1\text{H}$  HSQC spectrum of the MBP/β-cyclodextrin complex. Peaks assigned to backbone amides are labeled by residue number, while those tentatively assigned to side-chain  $\text{NH}_2$  and Trp side-chain indole protons are designated by \* and W, respectively.

amino acids, whereas intraresidue correlations were noted for 94.6 and 93.7% of non-Pro residues in HNCA and HN(CA)CB spectra, respectively. Similarly, complete HN(CO)CA and HN(COCA)CB data were obtained with 94.6 and 94.0% of the possible correlations observed, respectively. It is worth emphasizing that all of the spectra were recorded at 37 °C and at this temperature  $^{15}\text{N}$  relaxation measurements<sup>39</sup> of the MBP/β-cyclodextrin complex indicate an overall correlation time of 16.2 ± 1.0 ns.

Aside from improving the sensitivity of these triple resonance methods, the decreased  $^{13}\text{C}$  relaxation rates in highly deuterated systems facilitate the use of constant-time spectroscopy to record  $^{13}\text{C}$  chemical shifts, providing a number of benefits in the analysis of spectra of large proteins. Most importantly, as discussed in detail previously,<sup>8,13</sup> CT-based methods offer significantly better resolution than their non-CT counterparts. This is particularly critical in the analysis of spectra of molecules with close to 400 residues, such as in the case of MBP, and enables the resolution of peaks separated in the  $^{13}\text{C}$  dimension by as little as 0.4 ppm. This is shown in Figure 4b, where correlations to valine  $\text{C}\beta$  nuclei (circled) show a main peak flanked by a weak upfield shoulder with intensity of 13 ± 6% of the main peak, corresponding to Val residues with  $\text{CD}(\text{CH}_3)_2$  and  $\text{CD}(\text{CD}_3)_2$  side chains, respectively. For each Val, these two peaks are well-resolved despite the small chemical shift difference between them ( $\Delta\delta = 0.48 \pm 0.02$  ppm). The increased resolution provided by CT-based spectroscopy is particularly crucial in establishing connections between sequential residues that have similar  $^{13}\text{C}\alpha$  or  $^{13}\text{C}\beta$  chemical shifts. This is illustrated in Figure 5 with slices from the  $\text{C}\beta$ -directed CT-HN(COCA)CB and CT-HN(CA)CB experiments where one can clearly distinguish peaks separated by approximately 0.4 ppm. It is important to emphasize that these CT methods require high levels of deuteration; with fully protonated systems, unacceptable

sensitivity losses occur from relaxation during relatively long constant-time periods. In this regard it is noteworthy that in the case of the CT-HN(COCA)CB and CT-HN(CA)CB experiments, complete or near-complete levels of deuteration at both the  $\text{C}\alpha$  and  $\text{C}\beta$  positions are necessary.<sup>8,13</sup>

In addition to improved resolution, CT-HN(COCA)CB and CT-HN(CA)CB experiments also provide valuable assignment information encoded in the sign of cross-peaks. As discussed previously,<sup>13</sup> evolution of  $^{13}\text{C}\beta$  magnetization from one-bond  $^{13}\text{C}-^{13}\text{C}$  scalar couplings during the carbon constant-time evolution period leads to a modulation of the signal intensity according to  $\cos^N(\pi J_{\text{CC}}T_{\text{C}})$  where  $T_{\text{C}}$  is the length of the constant-time period and  $N$  is the number of aliphatic  $^{13}\text{C}$  nuclei attached to the carbon of interest. Thus by choosing  $T_{\text{C}} = 1/J_{\text{CC}}$ , cross-peaks from  $\text{C}\beta$  carbons with an even number of attached aliphatic carbons are of opposite phase relative to peaks originating from residues with an odd number of aliphatic carbons attached to the  $\text{C}\beta$  position. By combining this sign information along with a comparison of the observed  $\text{C}\alpha/\text{C}\beta$  shifts to the average  $\text{C}\alpha$  and  $\text{C}\beta$  shifts of the 20 amino acids,<sup>40</sup> we were able to quickly make residue-specific assignments throughout most of the protein.

On the basis of the CT-HNCA, CT-HN(CO)CA, CT-HN(CA)CB, and CT-HN(COCA)CB experiments, a total of 96.5% (95.6%) of all  $^{13}\text{C}\alpha$  ( $^{13}\text{C}\beta$ ) chemical shifts were assigned along with a comparable fraction of  $^{15}\text{N}-^1\text{H}$  pairs (94.6% of all non-proline amino acids). A slightly lower fraction of  $^{13}\text{C}$  shifts were assigned (89.2%) based solely on HNCO data. This lower number reflects the fact that the shifts of the carbonyl carbons of the 21 amino acids N-terminal to proline residues cannot be obtained from the HNCO experiment. The majority of the missing assignments cluster in one section from P229 to K239, where cross-peaks were not observed in spectra. Cross-peaks from two other regions that are close to this segment either in primary sequence (V240–Y242) or tertiary structure (A215–

(39) Farrow, N. A.; Muhandiram, D. R.; Singer, A. U.; Pascal, S. M.; Kay, C. M.; Gish, G.; Shoelson, S. E.; Pawson, T.; Forman-Kay, J. D.; Kay, L. E. *Biochemistry* **1994**, 33, 5984–6003.

(40) Seavy, B. R.; Farr, E. A.; Westler, W. M.; Markley, J. L. *J. Biomol. NMR* **1991**, 1, 217–236.

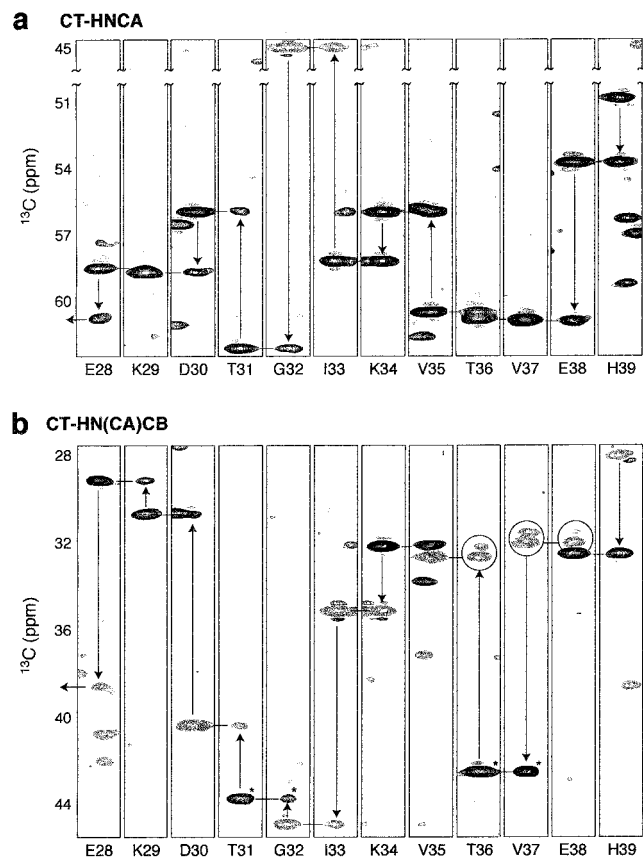


**Figure 4.** Representative slices from CT-HNCA (a) and CT-HN(CA)CB (b) spectra used in backbone  $^{13}\text{C}$  chemical shift assignment. Each  $F_1(^{13}\text{C}) - F_3(^1\text{HN})$  slice is labeled by the  $F_2$  frequency of the slice. Circled HN(CA)CB peaks arise from correlations to Val  $\text{C}^\beta$  nuclei. The weak upfield ( $F_1$ ) shoulders associated with the main peaks arise from the presence of a small fraction of valine residues with  $^{13}\text{CD}_3$  methyl groups ( $\approx 10\%$ ) as discussed in the text. Positive peaks are drawn with black contours, negative peaks with gray. Peaks marked with an asterisk (\*) are aliased in  $F_1$ .

A216) were of low intensity in spectra recorded for backbone assignment. All of these residues are in proximity to the bound  $\beta$ -cyclodextrin,<sup>41,42</sup> suggesting that conformational heterogeneity of residues in the binding site could be responsible for the missing cross-peaks. This is supported by  $^3\text{H}$  NMR studies that have established that significant conformational mobility exists within the MBP maltodextrin binding site.<sup>43</sup> It is noteworthy that broadening has been observed in ligand-binding regions of other proteins.<sup>14</sup>

**Side-Chain Assignments.** Once the backbone  $^{15}\text{N}$ ,  $^{13}\text{Ca}$ ,  $^1\text{HN}$ , and side chain  $^{13}\text{C}^\beta$  chemical shifts were obtained, assignment of methyl  $^1\text{H}$  and  $^{13}\text{C}$  shifts of Val, Leu, and Ile ( $\text{C}\delta 1$ ) residues followed. Central to this effort was the high efficiency and specificity of methyl protonation provided by the  $^{15}\text{N}, ^{13}\text{C}, ^2\text{H}$  ( $^1\text{H}$ -methyl)-labeling protocol (Figure 1). This resulted in the production of samples of MBP with protonated Val, Leu, and Ile  $\delta 1$  methyl groups<sup>20</sup> in an otherwise highly deuterated background. The specificity of the protonation in these samples is nicely illustrated in a comparison of CT  $^{13}\text{C}$ – $^1\text{H}$  HSQC spectra recorded on protonated and deuterated,

(41) Spurlino, J. C.; Liu, G.-Y.; Quiocho, F. A. *J. Biol. Chem.* **1991**, 266, 5202–5219.

(42) Scharff, A. J.; Rodseth, L. E.; Quiocho, F. A. *Biochemistry* **1993**, 32, 10553–10559.

(43) Gehring, K.; Williams, P. G.; Pelton, J. G.; Morimoto, H.; Wemmer, D. E. *Biochemistry* **1991**, 30, 5524–5531.

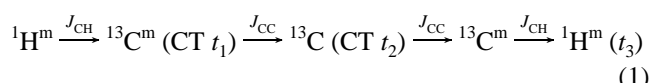
methyl-protonated samples (Figure 6). This comparison also shows that the reduction of proton–proton dipolar and scalar couplings in such highly deuterated samples leads to a significant narrowing of the methyl  $^1\text{H}$  line widths (from  $23.6 \pm 1.8$  Hz [ $^1\text{H}$ ] to  $16.5 \pm 1.2$  Hz [ $^2\text{H}$ ,  $^1\text{H}$ -methyl] for Ile  $\delta 1$ , with comparable results for Val and Leu). Figure 6 also shows that Leu methyl groups are relatively underprotonated in the  $^2\text{H}$ ,  $^1\text{H}$ -methyl sample, as discussed in the Materials and Methods section.

In contrast to the case of perdeuterated samples, where experiments for side-chain assignment must of necessity begin with magnetization on side-chain carbon spins,<sup>11</sup> the high degree of protonation on the methyl groups of Val, Leu, and Ile ( $\text{C}\delta 1$ ) residues in samples produced with the scheme of Figure 1 allows the use of experiments where signal originates on protons. Because intervening carbons between the protonated methyl groups and side-chain backbone positions are highly deuterated, magnetization can be relayed from the methyl position to the backbone  $^{15}\text{N}$ ,  $^1\text{HN}$  spins in a very efficient manner.<sup>28</sup>

Side-chain methyl correlations were obtained from a suite of  $^{13}\text{C}$ – $^{13}\text{C}$  TOCSY-based experiments which have been optimized for use with deuterated, methyl-protonated proteins. Experiments include the (H)C(CO)NH-TOCSY,<sup>28</sup> which links methyl  $^{13}\text{C}$  chemical shifts of residue  $i$  ( $^{13}\text{C}^m_i$ ) with  $^{15}\text{N}/^1\text{HN}$  shifts of residue  $i+1$  ( $^{15}\text{N}_{i+1}, ^1\text{HN}_{i+1}$ ), the H(CCO)NH-TOCSY ( $^{1\text{H}}_m, ^{15}\text{N}_{i+1}, ^1\text{HN}_{i+1}$  correlations) and the (H)C(CA)NH-TOCSY ( $^{13}\text{C}^m_i, ^{15}\text{N}_i, ^1\text{HN}_i$ , and  $^{13}\text{C}^m_i, ^{15}\text{N}_{i+1}, ^1\text{HN}_{i+1}$  correlations). The latter experiment was performed in order to obtain methyl shifts of residues that immediately precede Pro. Figure 7 presents strips from the (H)C(CO)NH-TOCSY and H(CCO)NH-TOCSY data sets, illustrating the high sensitivity of the experiments.

Although the TOCSY-based experiments described above allow the assignment of  $^{13}\text{C}$  and  $^1\text{H}$  methyl chemical shifts to specific Val, Leu, and Ile residues, in the case of Val and Leu they do not a priori establish which pairs of  $^{13}\text{C}^m, ^1\text{H}^m$  shifts correspond to a given methyl group. This information could be obtained from a 4D HC(CO)NH-TOCSY;<sup>44</sup> however, we prefer to use a new experiment, the (HM)CMC(CM)HM, which correlates chemical shifts of the methyl proton and carbon with the shift of the carbon adjacent to the methyl group. One particular advantage of this new experiment relates to its higher sensitivity relative to the 4D HC(CO)NH-TOCSY method.

Figure 8 illustrates the (HM)CMC(CM)HM pulse scheme that was developed. The sequence is comprised of elements that have been described in detail previously in the literature, and we therefore provide only a brief description here. The magnetization transfer steps in the pulse scheme can be schematically diagrammed as



where  $^1\text{H}^m$ ,  $^{13}\text{C}^m$ , and  $^{13}\text{C}$  are methyl protons, methyl carbons, and the methylene/methine carbons that are adjacent to methyl carbons,  $J_{\text{CH}}$  and  $J_{\text{CC}}$  are the scalar couplings active in each transfer step,  $t_i$  ( $i = 1–3$ ) is an acquisition time, and CT  $t_i$  is a constant-time indirect acquisition period. Fourier transformation of the resultant data set gives rise to cross-peaks at  $(\omega_{\text{C}}^m, \omega_{\text{C}}, \omega_{\text{H}}^m)$ .

As indicated in eq 1, magnetization originating on methyl protons is transferred to the directly attached carbons and the carbon chemical shift recorded in a constant-time manner for a

(44) Logan, T. M.; Olejniczak, E. T.; Xu, R. X.; Fesik, S. W. *FEBS Lett.* **1992**, 314, 413–418.

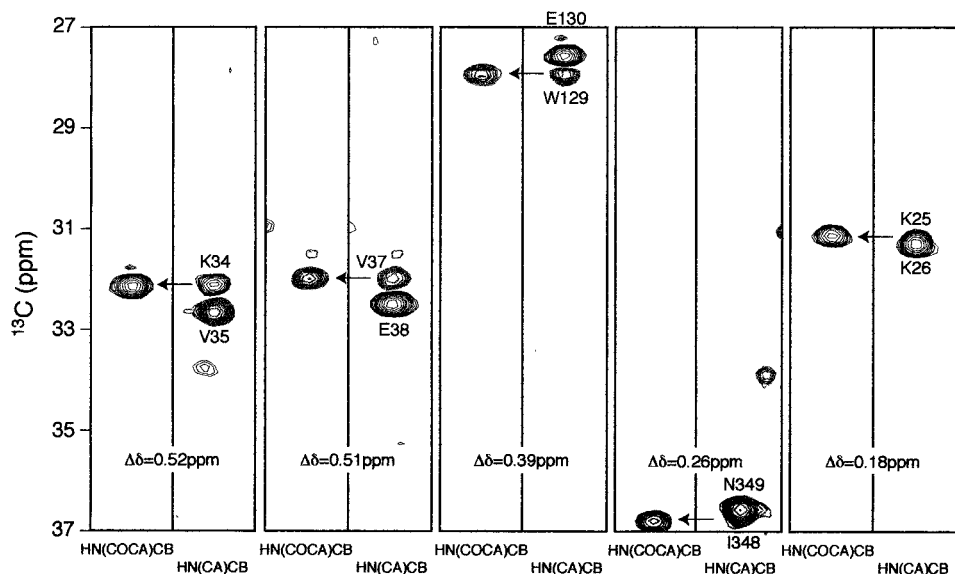


**Figure 5.** Utility of high-resolution CT-HN(CA)CB and CT-HN(COCA)CB spectra in correlating sequential residues with poor  $^{13}\text{C}\beta$  chemical shift separation. Slices from each experiment were taken at the  $^{15}\text{N}$ ,  $^1\text{H}$  shifts of the C-terminal residue in the pair of residues listed on each HN(CA)CB strip.  $\Delta\delta$  is the difference in  $^{13}\text{C}$  chemical shifts between the  $\text{C}\beta$  nuclei of the two sequential residues. Positive and negative cross-peaks are drawn with black and gray contours, respectively.

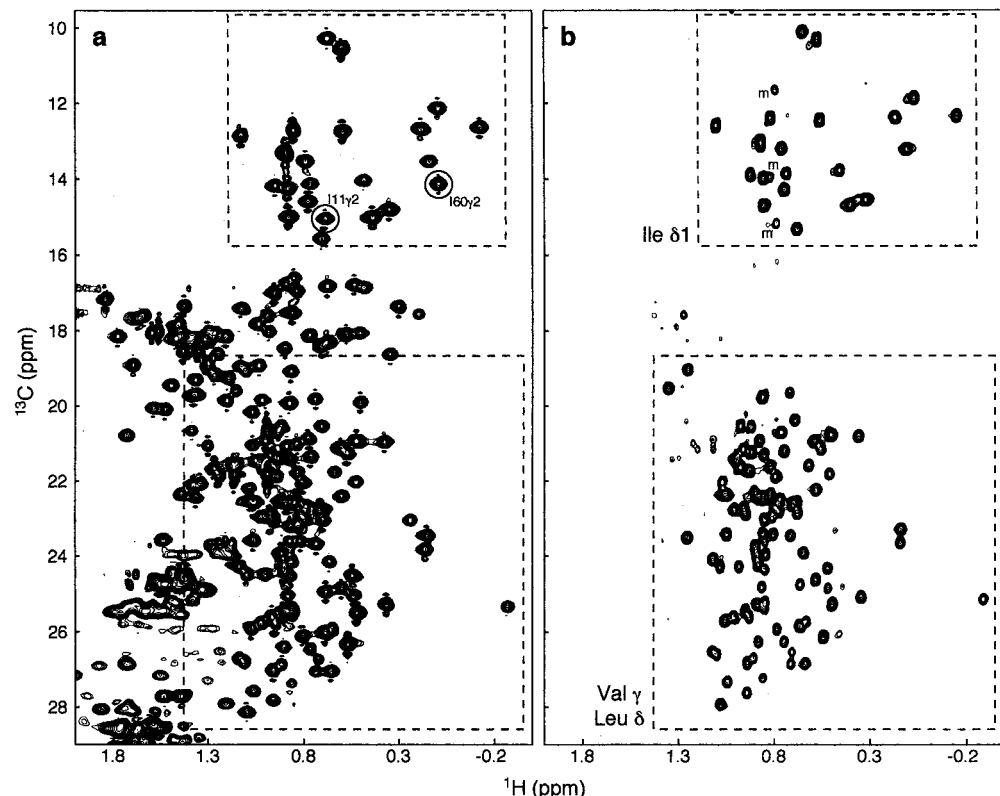


**Figure 6.** Efficiency and selectivity of  $^2\text{H}$  ( $^1\text{H}$ -methyl)-labeling at side chain positions. CT  $^{13}\text{C}$ – $^1\text{H}$  HSQC spectra were acquired on MBP/ $\beta$ -cyclodextrin complexes, using  $^{13}\text{C}$ ,  $^1\text{H}$ -(a) or  $^{13}\text{C}$ ,  $^2\text{H}$  ( $^1\text{H}$ -methyl)-labeled MBP. Spectra are plotted at equivalent levels, accounting for differences in sample concentration. Two Ile  $\gamma$ 2 cross-peaks (circled) with upfield  $^{13}\text{C}$  chemical shifts are located in the Ile  $\delta$ 1 box of spectrum a. Peaks marked with an m in spectrum b are from a small fraction of maltose-bound MBP ( $\approx 5\%$ ) present in the sample after the  $\beta$ -cyclodextrin exchange step.

duration of  $T \approx 1/2J_{\text{CC}}$ . During this period, evolution of magnetization due to the one-bond  $^{13}\text{C}$ – $^{13}\text{C}$  coupling occurs so that immediately prior to the  $^{13}\text{C}$  90° pulse of phase  $\phi_3$ , the signal of interest is given by  $\text{H}^m_z \text{C}^m_x \text{C}_z$ , where  $X_i$  corresponds to the  $i$  component of  $X$  magnetization. Subsequent application of the 90° $\phi_3$  pulse creates signal of the form  $\text{H}^m_z \text{C}^m_z \text{C}_x$ , which evolves for a period of  $2T$  during the second constant-time acquisition interval, extending from a to b in Figure 8.

Magnetization is returned to the methyl proton for detection by retracing the steps described above. A number of additional features of the pulse scheme are noteworthy. Correlations from Val are readily separated from cross-peaks originating from Leu or Ile using a scheme in which spectra are recorded with the  $^{13}\text{C}\alpha$  selective pulse applied at either point A or B in Figure 8. Note that during the  $2T$  ( $\sim 1/J_{\text{CC}}$ ) period  $^{13}\text{C}$  magnetization evolves from homonuclear couplings originating from each

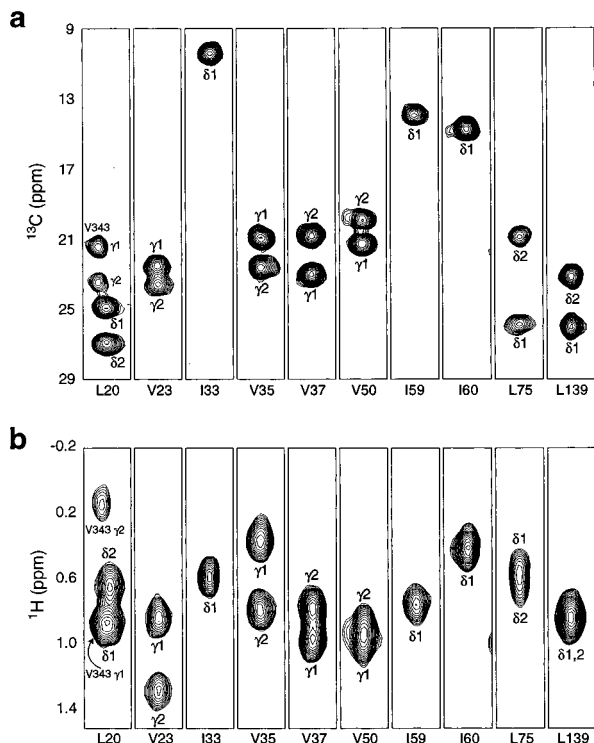


**Figure 7.** (H)C(CO)NH-TOCSY (a) and H(C(CO)NH-TOCSY (b) spectra of the  $^{15}\text{N}$ ,  $^{13}\text{C}$ ,  $^2\text{H}$  ( $^1\text{H}$ -methyl)-MBP/β-cyclodextrin complex. Strips are labeled with the identity of the methyl-containing residue.

directly coupled carbon spin. In the case of Val residues, the selective  $^{13}\text{C}\alpha$  pulse at point A results in a net refocusing of the evolution due to  $J_{\text{C}\alpha\text{C}\beta}$  for the  $2T$  interval. In contrast, if the selective pulse is applied at position B in the sequence, evolution from  $J_{\text{C}\alpha\text{C}\beta}$  proceeds for the entire  $2T$  period, inverting the sign of the magnetization at point b. The signals from Leu and Ile are not affected by the  $^{13}\text{C}\alpha$  selective pulses. Hence, linear combinations of the A and B experiments provide subspectra containing cross-peaks from only Val (A - B) or Leu/Ile( $\delta 1$ ) (A + B). A second point of note is that a  $^1\text{H}$   $180^\circ$  pulse is included after an interval of  $t_2/2 + \tau_b$  from the start of the second constant-time period. This pulse eliminates signal originating from molecules where carbons adjacent to methyl groups have small levels of residual protonation.<sup>26</sup> It is important to emphasize that we have no evidence to suggest residual protonation at carbon positions on methyl-containing residues in samples that have been prepared according to Figure 1.

The utility of this experiment is demonstrated in Figure 9 where several slices from the (HM)CMC(CM)HM data set recorded on the MBP/β-cyclodextrin complex are illustrated. The combination of the two  $^{13}\text{C}$  constant-time indirect detection periods and residue-specific editing provides spectra that are relatively free of cross-peak overlap, critically important for the successful analysis of data from a molecule containing 122 Val, Leu, and Ile ( $\delta 1$ ) methyl groups. On the basis of results from the (HM)CMC(CM)HM experiment alone, many of the Val methyl groups could be assigned by comparing  $^{13}\text{C}\beta$  chemical shifts obtained from this experiment with the Val  $^{13}\text{C}\beta$  assignments previously generated as part of the backbone assignment. The assignment of the remaining Val and of all of the Leu and Ile ( $\delta 1$ ) residues was achieved using data from the TOCSY-based experiments described above and the (HM)CMC(CM)-HM. The combination of data from the TOCSY-based and (HM)CMC(CM)HM experiments was particularly valuable for

Val and Leu residues which have at least one methyl group with chemical shifts within 0.2 ppm ( $^{13}\text{C}$ ) or 0.05 ppm ( $^1\text{H}$ ) of other methyls in  $^{13}\text{C}$ - $^1\text{H}$  HSQC spectra (approximately 50% of the Val and Leu in the MBP/β-cyclodextrin complex). In these cases, the resolution in the methyl carbon and proton dimensions of the TOCSY-based experiments may not be sufficient to uniquely identify a single  $^{13}\text{C}$ - $^1\text{H}$  HSQC cross-peak. These ambiguities were resolved using (HM)CMC(CM)-HM spectra, taking advantage of the high resolution afforded by the  $^{13}\text{C}\beta$  (Val) or  $^{13}\text{C}\gamma$  (Leu) chemical shifts.

In total, 119 of the 122 Val, Leu, and Ile ( $\delta 1$ ) methyl groups were assigned in the MBP/β-cyclodextrin complex (Figure 10). The three missing methyl groups are from two residues (Ile 235, Val 240) that are in an exchange-broadened region of the  $^{15}\text{N}$ - $^1\text{H}$  HSQC, where  $^{15}\text{N}$ - $^1\text{H}$  correlations are either very weak or are not observed. We have tentatively assigned a  $^{13}\text{C}$ - $^1\text{H}$  HSQC peak to the Val 240 $\gamma 1$  methyl group since the  $^{13}\text{C}$  and  $^1\text{H}$  chemical shifts of this cross-peak are in the region of the spectrum where Val methyls are found and since all of the other peaks in this region were accounted for. The stereospecific assignment of this methyl was obtained from the sign of its cross-peak in a  $^{13}\text{C}$ - $^1\text{H}$  HSQC spectrum recorded on a 10%  $^{13}\text{C}$ -labeled sample.<sup>25</sup> Finally, assignment of the Leu C $\gamma$  and Ile C $\gamma 1$  carbons followed directly from the (HM)CMC(CM)-HM spectrum, once the identity of all of the methyl peaks was established. Table 2 in Supporting Information provides a listing of all of the  $^{15}\text{N}$ ,  $^{13}\text{C}\alpha$ ,  $^{13}\text{C}\beta$ , and  $^1\text{H}$  shifts as well as of the methyl  $^1\text{H}$  and  $^{13}\text{C}$  chemical shifts of Val, Leu, and Ile (C $\delta 1$ ) residues in the MBP/β-cyclodextrin complex.

**Analysis.** The chemical shift assignments that we have obtained form the basis for identifying structural elements within the MBP/β-cyclodextrin complex through an analysis of the deviations of the observed  $^{13}\text{C}\alpha$  and  $^{13}\text{C}\beta$  chemical shifts from their residue-dependent random coil values.<sup>35,36,45</sup> In Figure 11a, the parameter  $(\Delta C^\alpha - \Delta C^\beta)_{\text{smoothed}}$ <sup>36</sup> is plotted for each residue for which chemical shift data is available. Multiple regions are observed where consecutive  $(\Delta C^\alpha - \Delta C^\beta)$  values exceed a threshold level, identifying helical [ $(\Delta C^\alpha - \Delta C^\beta) > 1.4$ ] and strand [ $(\Delta C^\alpha - \Delta C^\beta) < 1.4$ ] secondary structure elements. Examining the locations of these elements (Figure 11b) shows them to be well correlated with the positions of comparable structural elements in a 1.8 Å crystal structure of the MBP/β-cyclodextrin complex (Figure 11c).<sup>42</sup>

Additional information on the presence of secondary structure elements is provided by qualitative  $^2\text{H}$ - $^1\text{H}$  exchange protection data that can be easily obtained from highly deuterated proteins. When such proteins are biosynthetically produced in  $\text{D}_2\text{O}$ -rich media, all of the exchangeable sites (including backbone amides) are fully deuterated. Many of these sites become protonated by exchange processes during the subsequent purification in  $\text{H}_2\text{O}$ -based buffers. However, a significant number of backbone amides (approximately 50 in our system) exchange too slowly during the purification process (4 °C, 7–10 days) to become highly protonated, suggesting that these sites are protected from exchange by their involvement in stable hydrogen bonds as might be found in elements of regular secondary structure. Exchange protection was assessed in a qualitative manner by recording two  $^{15}\text{N}$ - $^1\text{H}$  HSQC spectra of the MBP/β-cyclodextrin complex, one prior to the guanidinium unfolding/refolding step in our sample preparation and one afterward. Residues that were absent or severely attenuated in the first spectrum (compared to the second) were scored as protected and are indicated with dots in Figure 11b. Most of these protected

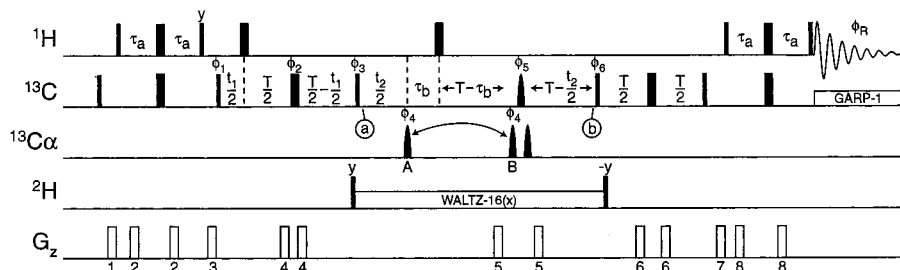


**Figure 8.** Pulse sequence for the (HM)CMC(CM)HM experiment. All narrow (wide) rectangular pulses have flip angles of  $90^\circ$  ( $180^\circ$ ).  $^1\text{H}$ ,  $^{13}\text{C}$ , and  $^2\text{H}$  rectangular pulses are centered at 4.66 (water), 25.0, and 2.5 ppm, respectively, and are applied with 31, 21, and 1.9 kHz rf fields, respectively. The single shaped pulse (350  $\mu\text{s}$ ) on the  $^{13}\text{C}$  channel has the RE-BURP profile<sup>48</sup> and is centered at 38 ppm by a 13 ppm phase-modulation of the carrier frequency.<sup>49,50</sup> Note that this pulse is of sufficient strength to cover the entire range of aliphatic  $^{13}\text{C}$  chemical shifts. The  $^{13}\text{Ca}$  selective pulses are 1.3 ms long and have the I-BURP2 profile<sup>48</sup> with a center of excitation at 62.5 ppm (37.5 ppm modulation of the carrier).  $^2\text{H}$  decoupling was achieved using a 0.7 kHz WALTZ-16 field,<sup>51</sup> whereas  $^{13}\text{C}$  decoupling during acquisition employed a 2.2 kHz GARP-1 field.<sup>52</sup>  $^2\text{H}$  decoupling is interrupted prior to the application of gradient pulses.<sup>53</sup> The location of the first  $^{13}\text{Ca}$  selective pulse was alternated between points A and B and data recorded in an interleaved manner. Postacquisition combination of FIDs from experiments recorded with the pulse at A and B was achieved using in-house written software. The following delays were used:  $\tau_a = 1.9$  ms,  $T = 14.5$  ms ( $\approx 1/2J_{\text{CC}}$ ) and  $\tau_b = 1.92$  ms. The phase cycle employed is:  $\phi_1 = (x, -x)$ ;  $\phi_2 = x$ ;  $\phi_3 = 2(y), 2(-y)$ ;  $\phi_4 = 2(x), 2(-x)$ ;  $\phi_5 = 4(x), 4(-x)$ ;  $\phi_6 = 4(y), 4(-y)$ ;  $\phi_R = (x, -x)$ .  $F_1$  and  $F_2$  quadrature detection was achieved by States-TPPI<sup>54</sup> of  $\phi_1$  ( $F_1$ ) and of  $\phi_1, \phi_2, \phi_3$  ( $F_2$ ), respectively. The duration and strengths of the gradients are  $g1 = (500$   $\mu\text{s}$ , 10 G/cm);  $g2 = (400$   $\mu\text{s}$ , 5 G/cm);  $g3 = (1$  ms, 15 G/cm);  $g4 = (200$   $\mu\text{s}$ , 18 G/cm);  $g5 = (600$   $\mu\text{s}$ , 10 G/cm);  $g6 = (500$   $\mu\text{s}$ , 5 G/cm);  $g7 = (800$   $\mu\text{s}$ , 8 G/cm) and  $g8 = (200$   $\mu\text{s}$ , 3 G/cm). The  $^2\text{H}$  lock channel is interrupted at the start of each transient and re-engaged immediately prior to acquisition.

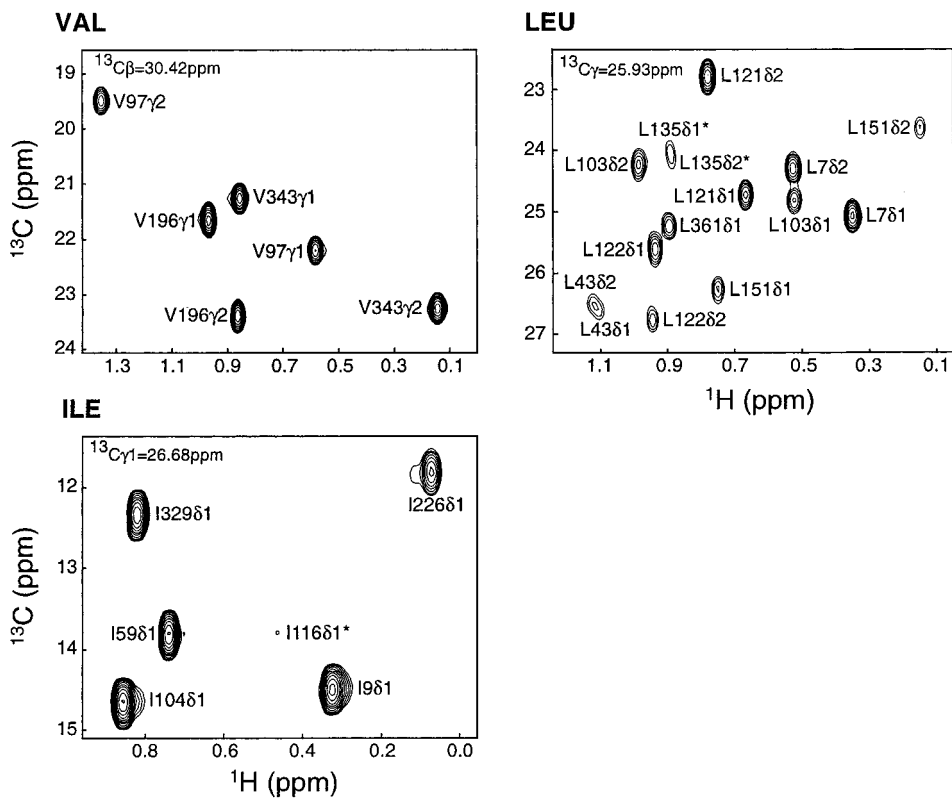


**Figure 9.** (HM)CMC(CM)HM spectra of the  $^{15}\text{N}, ^{13}\text{C}, ^2\text{H}$  ( $^1\text{H}$ -methyl)-MBP/ $\beta$ -cyclodextrin complex. Regions of  $F_1$  ( $^{13}\text{C}^m$ )– $F_3$  ( $^1\text{H}^m$ ) slices are illustrated from planes with the  $F_2$  frequency indicated at the top of each slice. Peaks marked with \* are more intense on an adjacent  $F_2$  plane.

residues are located in secondary structure elements identified by analysis of the  $(\Delta C^\alpha - \Delta C^\beta)_{\text{smoothed}}$  parameter or from the X-ray structure of the MBP/ $\beta$ -cyclodextrin complex.

### Concluding Remarks

Using the  $^{15}\text{N}, ^{13}\text{C}, ^2\text{H}$  ( $^1\text{H}$ -methyl)-labeling protocol described in Figure 1 in concert with a suite of triple resonance, multidimensional experiments optimized for use with such samples, we have been able to assign the chemical shifts of virtually all of the  $^{15}\text{N}$ ,  $^{13}\text{Ca}$ ,  $^{13}\text{C}\beta$ , and  $^1\text{H}$  nuclei in the 370

residue MBP component of a 42 kDa MBP/ $\beta$ -cyclodextrin complex. Near complete assignments for the methyl carbon and proton chemical shifts of Val, Leu, and Ile ( $\text{C}\delta 1$ ) residues have been obtained as well. These chemical shift assignments were made in the absence of any information derived from the crystal structure of this complex.<sup>42</sup> This structure was examined only after the assignment was completed, allowing a comparison of the NMR- and crystallographically determined locations of secondary structure elements within the protein. In addition, analysis of the crystal structure proved useful for rationalizing

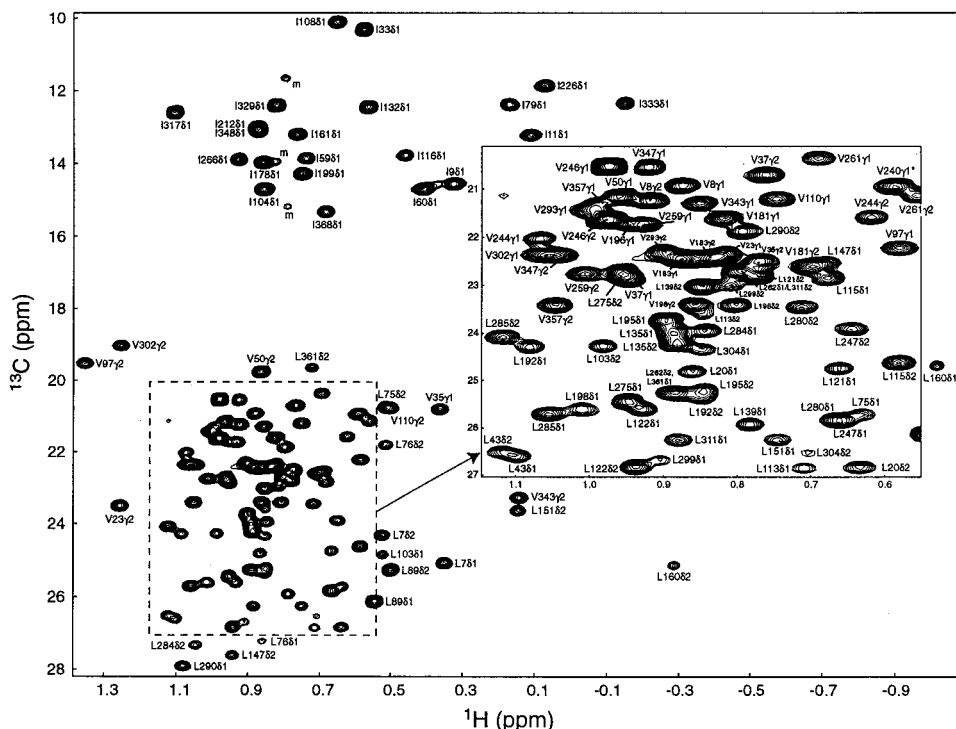


**Figure 10.** CT  $^{13}\text{C}$ – $^1\text{H}$  HSQC of the  $^{15}\text{N}$ , $^{13}\text{C}$ , $^2\text{H}$  ( $^1\text{H}$ -methyl)-MBP/ $\beta$ -cyclodextrin complex. Cross-peaks are labeled with their assignments; the V240 $\gamma$ 1 assignment is tentative (see text) and is therefore labeled with \*. Peaks marked with an m are from a small fraction of maltose-bound MBP (~5%) present in the sample after the  $\beta$ -cyclodextrin exchange step.

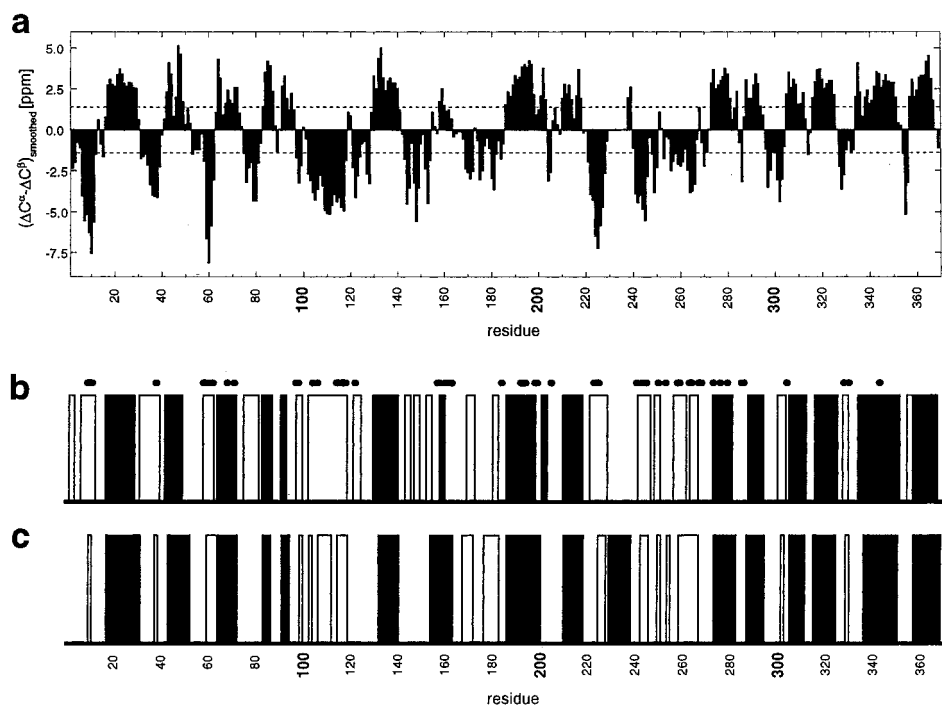


**Figure 11.** Identification of secondary structure elements in the MBP/β-cyclodextrin complex by NMR chemical shift methods. (a)  $(\Delta C^\alpha - \Delta C^\beta)_{\text{smoothed}}$  index plot.<sup>36</sup> The dashed lines indicate the 1.4 ppm threshold for identification of secondary structure elements. (b,c) Comparison of the secondary structure elements identified by the  $(\Delta C^\alpha - \Delta C^\beta)$  index (b) and those in the crystal structure of the MBP/β-cyclodextrin complex (c) (PDB code 1dmb<sup>42</sup>). Helical and strand segments are indicated by filled and unfilled bars, respectively. The secondary structure assignments used in panel c were made with the program MOLMOL.<sup>55</sup> The dots in panel b indicate residues protected from HN exchange as determined by a qualitative analysis of  $^{15}\text{N}-^1\text{H}$  HSQC spectra recorded on the MBP/β-cyclodextrin complex before and after the unfolding/refolding step described in Materials and Methods.

the locations of the few nonassigned regions in light of possible ligand-related exchange processes.

Our analysis here shows that MBP in this complex has a similar global structure in solution and crystalline forms, although local structural differences have been identified from ligand-related exchange processes.

NOE and heteronuclear coupling data.<sup>24</sup> With the backbone and side-chain chemical shifts of this complex now available, we are proceeding with the collection and assignment of NOE-based distance restraints. Here, the <sup>2</sup>H (<sup>1</sup>H-methyl)-labeling pattern provides the opportunity to obtain CH<sub>3</sub>–HN and CH<sub>3</sub>–

$\text{CH}_3$  distance restraints between residues that are widely separated in primary sequence. Central to this effort has been the development of a number of new NOESY experiments<sup>24,46</sup> that incorporate constant-time chemical shift evolution periods so that  $^{13}\text{C}$  chemical shifts can be recorded with high resolution. It is anticipated that the present labeling methodology and the NOE- and dipolar coupling<sup>47</sup>-based NMR experiments that have recently been developed will play an important role in facilitating NMR-based structural studies of proteins in the 35–50 kDa molecular weight range.

**Acknowledgment.** This research was supported by grants from the Medical Research Council of Canada to L.E.K. and K.G. We thank Dr. Ranjith Muhandiram (University of Toronto) for assistance in setting up many of the NMR experiments, Randall Willis (Hospital for Sick Children) and Natalie Goto

(46) Zwahlen, C.; Gardner, K. H.; Sarma, S. P.; Horita, D. A.; Byrd, R. A.; Kay, L. E. *J. Am. Chem. Soc.* **1998**, *120*, 7617–7625.  
 (47) Tjandra, N.; Bax, A. *Science* **1997**, *278*, 1111–1114.  
 (48) Geen, H.; Freeman, R. *J. Magn. Reson.* **1991**, *93*, 93–141.  
 (49) Boyd, J.; Sofje, N. *J. Magn. Reson.* **1989**, *85*, 406–413.  
 (50) Patt, S. L. *J. Magn. Reson.* **1992**, *96*, 94–102.  
 (51) Shaka, A. J.; Keeler, J.; Frenkel, T.; Freeman, R. *J. Magn. Reson.* **1983**, *52*, 335–338.

(University of Toronto) for preparation of samples used in this work, and Dr. Bruce Johnson (Merck) for providing scripts and advice regarding the use of NMRView. K.H.G. gratefully acknowledges a postdoctoral fellowship from the Helen Hay Whitney Foundation. L.E.K. is an International Howard Hughes Research Scholar.

**Supporting Information Available:** One table listing the experimental parameters used for the NMR experiments described in the text and a table listing the  $^{15}\text{N}$ ,  $^{13}\text{C}\alpha$ ,  $^{13}\text{C}\beta$ ,  $^1\text{H}$  chemical shifts as well as the methyl carbon and proton chemical shifts of Val, Leu, and Ile ( $\text{C}\delta 1$ ) residues of the MBP component (370 residues) of a 42 kDa MBP/ $\beta$ -cyclodextrin complex (10 pages, print/PDF.) See any current masthead page for ordering information and Web access instructions.

JA982019W

(52) Shaka, A. J.; Barker, P. B.; Freeman, R. *J. Magn. Reson.* **1985**, *64*, 547–552.  
 (53) Kay, L. E. *J. Am. Chem. Soc.* **1993**, *115*, 2055–2057.  
 (54) Marion, D.; Ikura, M.; Tschudin, R.; Bax, A. *J. Magn. Reson.* **1989**, *85*, 393–399.  
 (55) Koradi, R.; Billeter, M.; Wüthrich, K. *J. Mol. Graphics* **1996**, *14*, 51–55.